We are IntechOpen,
the world's leading publisher of
Open Access books
Built by scientists, for scientists

6,900
Open access books available

185,000
International authors and editors

200M
Downloads

154
Countries delivered to

Our authors are among the

TOP 1%
most cited scientists

12.2%
Contributors from top 500 universities

CLARIVATE ANALYTICS
BOOK CITATION INDEX
INDEXED

WEB OF SCIENCE™

Selection of our books indexed in the Book Citation Index
in Web of Science™ Core Collection (BKCI)

Interested in publishing with us?
Contact book.department@intechopen.com

An Approach for Estimating Geothermal Reservoir Productivity under Access Limitations Associated with Snowy and Mountainous Prospects

Mitsuo Matsumoto

Abstract

This chapter describes an approach to estimate reservoir productivity during the active exploration and development of a geothermal prospect. This approach allows a reservoir model to be updated by overcoming the severe time limitations associated with accessing sites for drilling and well testing under snowy and mountainous conditions. Performed in parallel with the conventional standard approach, the new approach enables us to obtain a first estimate of the reservoir productivity at an early time and to make successful project management decisions. Assuming a practical geothermal field, the procedures of the new approach are demonstrated here in detail. Finally, frequency distributions for the expected production rates and changes in the reservoir pressure at an arbitrary time are obtained during an assumed operational period.

Keywords: reservoir modeling, wellbore flow modeling, well testing, reservoir engineering, production engineering, project management

1. Introduction

The exploration and development lead time of a geothermal prospect directly affects its profitability because of the yearly interest factored into the cost. Sufficient profits purely produced by geothermal resources without financial support from other budgets are essential to enhance the development of environmentally friendly geothermal resources. This is why we cannot avoid trade-offs between exhaustively studying a geothermal reservoir and rapidly advancing a geothermal project.

Figure 1 shows an example of a fiscal annual schedule during an explorational and developmental project in which the author was involved as a reservoir engineer. The project was conducted in a snowy and mountainous area in northeastern Japan, where several geothermal projects have been conducted over the last decade [1]. In such areas, the schedules of drilling, well testing, and any other work at a site are
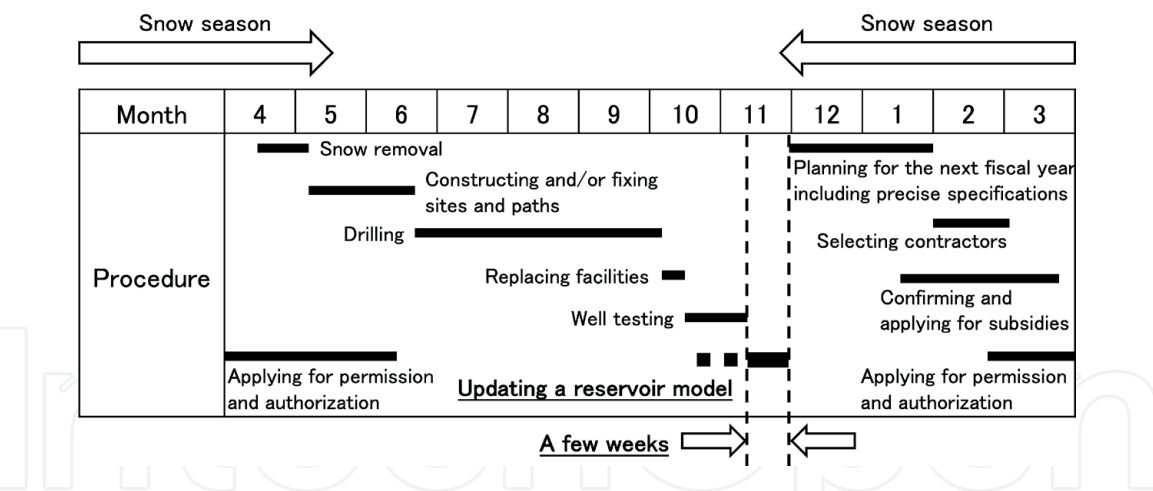
Figure 1.
Example of an annual schedule during an explorational and developmental project.

strictly limited by the snowy season. In addition, mountainous conditions limit the number of site locations that can satisfy the following conditions:

1. Accessibility to targets using directional or vertical drilling;

2. Sufficient space to install facilities for drilling and well testing;

3. Sufficient water supplies from nearby streams;

4. Accessibility to the site via paths constructed within realistic time and cost constraints including snow removal; and

5. The possibility of receiving permission and authorization while obeying numerous national regulations.

Under these severe limitations, project personnel usually identify a small number of possible locations following a large amount of effort, rather than easily selecting a location from a large number of options.

Geoscientists and engineers have only a few weeks to update a reservoir model by analyzing, considering, discussing, and updating their understanding of a geothermal system after collecting all the new data from a given year (**Figure 1**). Under such severe conditions, it is essential to account for the updated reservoir model when planning for the subsequent fiscal year. This chapter describes a concept and techniques to construct and update a reservoir model, as well as to estimate the reservoir productivity, by making the most of the highly limited time available during an active explorational and developmental project. The concept and techniques are based on the author's experience as a reservoir engineer in a real project even though specific information regarding the project, including the observational data, cannot be shown because of confidentiality reasons. The techniques described in this chapter have been partially reviewed and published in several articles and proceedings. This chapter focuses on practical procedures to construct a reservoir model by assembling these techniques.

2. Approaches to reservoir modeling

2.1 Standard approach

Let us begin by discussing the fundamental concept involved in conventional reservoir modeling approaches. As widely accepted and detailed in textbooks [2, 3],

the standard legitimate approach first involves the development of a conceptual model driven by several geological, hydrological, geophysical, and geochemical observations. This first step of the standard approach establishes the basis of the understanding of a geothermal system and requires exhaustive discussions that can comprehensively and consistently explain all the geoscientific observations. A good conceptual model plays a key role in successful reservoir modeling.

After the exhaustive study needed to construct a conceptual model, a natural-state model is developed to obey the principles of fluid dynamics, such as the conservation of mass and energy, as well as Darcy's law governing mass fluxes in a reservoir. Numerical reservoir simulators such as TOUGH2 [4] can be adopted in this and following steps. Steady-state fluid flow due to thermal convection is generally assumed in a reservoir. The natural-state model needs to reproduce the observed static temperature and pressure wireline logging data at the explorational wells while obeying the conceptual model. Calibration of the natural-state model to satisfy these requirements involves adjusting several conditions such as the permeability distributions and boundary conditions and often necessitates numerous trial runs of the reservoir simulator. After completing the natural-state modeling, the transient pressure and temperature responses in the reservoir during well testing are finally simulated to enable history matching and the forecasting of future operational scenarios. These later steps also require trial-and-error simulations and may require going back to earlier steps to reconsider and modify the model.

Planning for the next fiscal year, including decisions with respect to continuing or stopping the explorational and developmental project, as shown in **Figure 1**, requires both updates of the understanding of the geothermal system to determine drilling targets and estimates of the reservoir productivity to evaluate the project profitability. Following the abovementioned standard approach, we can obtain an update of the former at an early step, while an update of the latter becomes available after completion of the final step. As a result, estimates of reservoir productivity are strongly affected by the progress of earlier steps and are often delayed.

2.2 New approach

We can attempt another approach to overcome the difficulties causing delays in the reservoir productivity estimation by advancing inversely in parallel with the standard approach [5]. A comparison between the standard and new approaches is illustrated in **Figure 2**. The new approach first refers to the transient pressure responses during well testing, as well as the other transient responses of the temperature and tracer concentration if possible. In this step, we focus on reproducing these transient responses using a simple reservoir model.

The reservoir model may, at first, be very simple, represented by a single horizontal planar porous medium, as generally assumed in a conventional well test analysis (e.g., [6]). As the study progresses, the reservoir model is extended to become increasingly sophisticated and realistic by considering the dip and strike of the planar porous medium and three-dimensional connections between multiple planar porous media, as common in fracture reservoirs in Japan. The geometry and connectivity of the planar porous media are primarily based on direct observations, such as those made while drilling gend logging, as well as pressure interference and tracer testing, rather than referring to geological or other geoscientific interpretations. Once the observed transient responses are successfully reproduced, we can progress to forecasting future operational scenarios and obtain an estimate of the reservoir productivity (i.e., the possible steam and/or brine production rate during an assumed operational period). Appropriately calibrated wellbore models using production logging data are often combined with the reservoir model to forecast future scenarios.
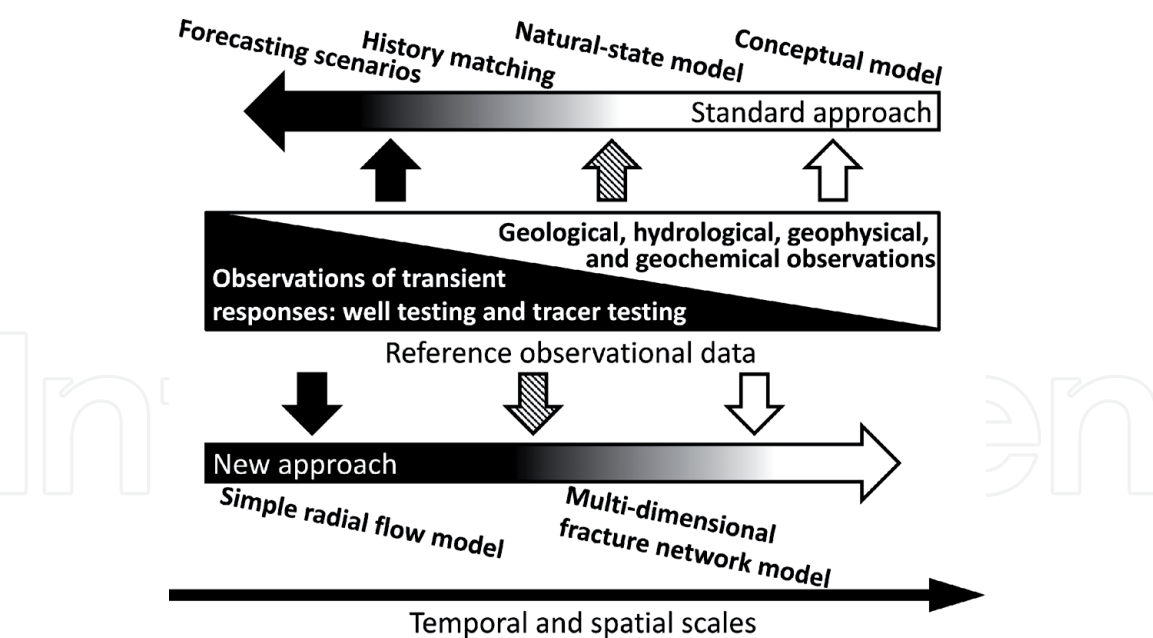
Figure 2.
Comparison between the standard and new approaches.

Accordingly, we can rapidly obtain a first estimate of the reservoir productivity by primarily referring to direct observations, a technique that is free of the conceptual and steady-state models considered in the standard approach. Referring to this estimate, a project manager can prepare a plan for the next fiscal year and make decisions concerning continuing or stopping the project in parallel with the ongoing standard approach. As the understanding of the geothermal system is improved with the standard approach, the reservoir model in the new approach evolves into an ever more sophisticated model that is consistent with the conceptual and natural-state models. The estimate of the reservoir productivity is also repeatedly updated. The estimates and their update history are reported continuously to the project manager; this is advantageous not only for successful project management but also for quantifying the impact of each estimate update. This new approach enables us to improve the efficiency and timeliness of estimating the reservoir productivity and to contribute to on-schedule project management.

3. Implementation

The author developed a mathematical model and numerical code to implement this new approach for a real explorational and developmental project [5]. Instead of a multi-purpose code designed to cover a wide range of conditions, the model and code were designed to be applicable to several specific projects in which the author was involved as a reservoir engineer. Therefore, a type of discrete fracture network model was adopted to represent a single-phase fracture reservoir. As often seen in geothermal prospects in Japan, the fracture network was assumed to be roughly distributed. In other words, at most, a countable number of large fractures or fractured zones with high permeability–thickness products totally or partially intersected a geothermal field (**Figure 3**). Wells in such geothermal fields intersect at most at a few fractures within their drilling depths of approximately 2000 m. Excepting these fractures, formation permeabilities tend to be very low to negligible. Representative examples of such reservoirs can be found in the Takigami [7] and Ogiri [8] fields in southwestern Japan. Each fracture or fractured zone in the model is represented
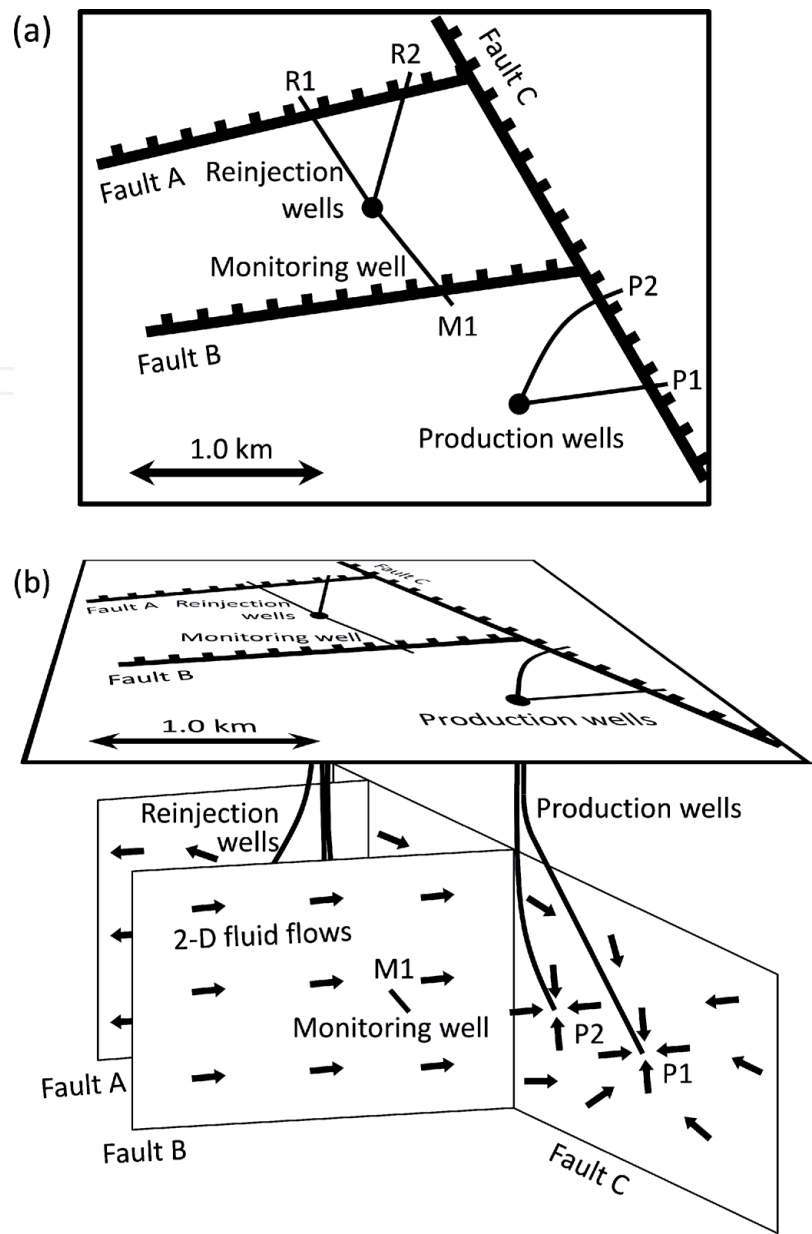
Figure 3.
Conceptual schematic of the reservoir model: (a) an assumed geothermal field and (b) a three-dimensional view of the fracture reservoir model beneath the assumed geothermal field.

by a planar porous medium with a relatively high permeability–thickness product of 10^{-11} m^2 or more. Formations, except fractures, allow only thermal conduction without mass flow.

Let us consider simulating the assumed reservoir illustrated in **Figure 3** as an example. The reservoir consists of three vertical fractures generated by Faults A–C that are represented by planar porous media with the dimensions shown in **Figure 4**. The vertical length of each fracture is assumed to be 2 km based on geological interpretations, while the horizontal length is assumed based on a specific concept of this approach discussed in Section 5. Several production, reinjection, and monitoring wells directionally intersect the fractures. The vertical initial pressure distribution obeys hydrostatic pressure with a specified value of 10 MPa at a depth of 1000 m from the top of the fractures. The initial distribution of the specific enthalpy is uniformly 1085.8 kJ/kg, which indicates an initial reservoir temperature of approximately 250 °C. The top and bottom boundaries of each fracture are modeled with impermeable and adiabatic boundary conditions, while the left boundary of each fracture and the right boundary of Fracture C maintain constant pressure and specific enthalpy values at the initial values.
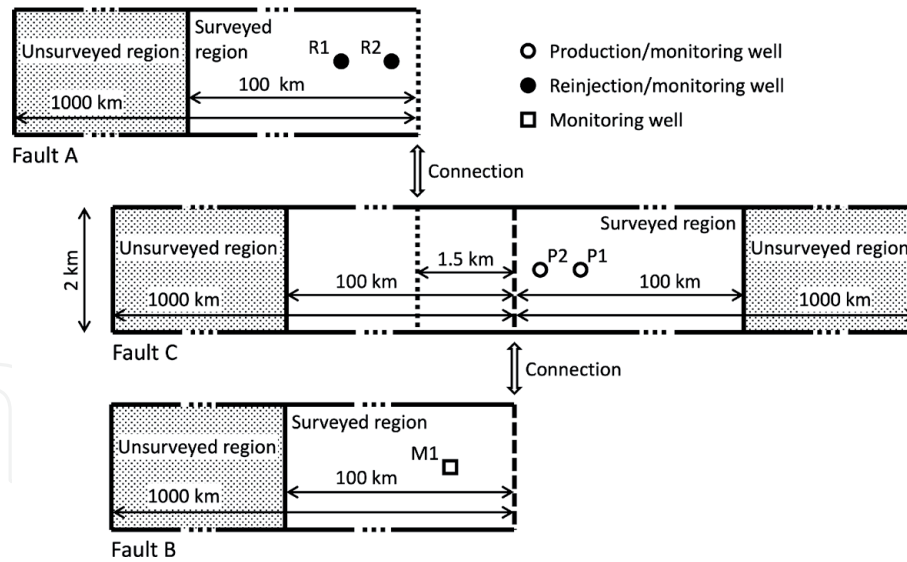
Figure 4.
Dimensions of the planar porous media representing faults A–C illustrated in **Figure 3**.

For both the surveyed and unsurveyed regions, the permeability, thickness, and porosity of each planar porous medium representing a fracture are set to 1.0×10^{-11} m^2, 5.0 m, and 20%, respectively, while the thermal conductivity and volumetric heat capacity are set to 3.0 W m^{-1} K^{-1} and 2.0×10^6 J m^{-3} K^{-1}, respectively. We assume that local thermal equilibrium between the fluid in the pores and the rock matrixes within a planar porous medium is reached immediately. This implies that the selection of the thickness value controls the heat exchange efficiency between the fluid and the formation under a constant thickness–porosity product value (i.e., the effective opening width of the fracture). For example, a case with a thickness of 1 m and a porosity of 10% and a case with a thickness of 10 m and a porosity of 1% have the same thickness–porosity product value of 0.1 m; however, the latter case has a larger heat exchange efficiency. This is because the volume of the rock matrix immediately exchanging heat with the fluid in the latter case is approximately 10 times larger than that in the former case. The one-dimensional conductive heat flux in the formation perpendicular to each fracture is also included. The grid size for the numerical simulation in each fracture is a uniform 100 m near the wells and expands exponentially in the horizontal direction.

First, we consider simulating a production test for a month using a production well P1, a reinjection well R1, and monitoring wells M1, P2, and R2. This problem addresses simulating the pressure interference observed at the monitoring wells by referring to the observed flow rates at the production and reinjection wells. We assume that the observed flow rates at P1 and R1 are constant at 250.0 t h^{-1} and 191.6 t h^{-1}, respectively, which implies that the produced reservoir fluid is separated into steam and water under a separator pressure of 0.35 MPaA (**Figure 5a**). The specific enthalpy of the reinjected water is assumed to be 561.5 kJ kg^{-1}, and the reinjected water is composed of saturated water at a pressure of 0.30 MPaA. Then, the pressure interference at each monitoring well is simulated, as shown in **Figure 5b**. In practice, for a real field, we would perform matching of the simulation results with the observations by adjusting parameters such as the permeability, thickness, and porosity of the planar porous media, as well as their network structure. In the cases encountered by the author at several real fields, simulations could accurately reproduce the observed pressure interference after a few tens of trial runs.
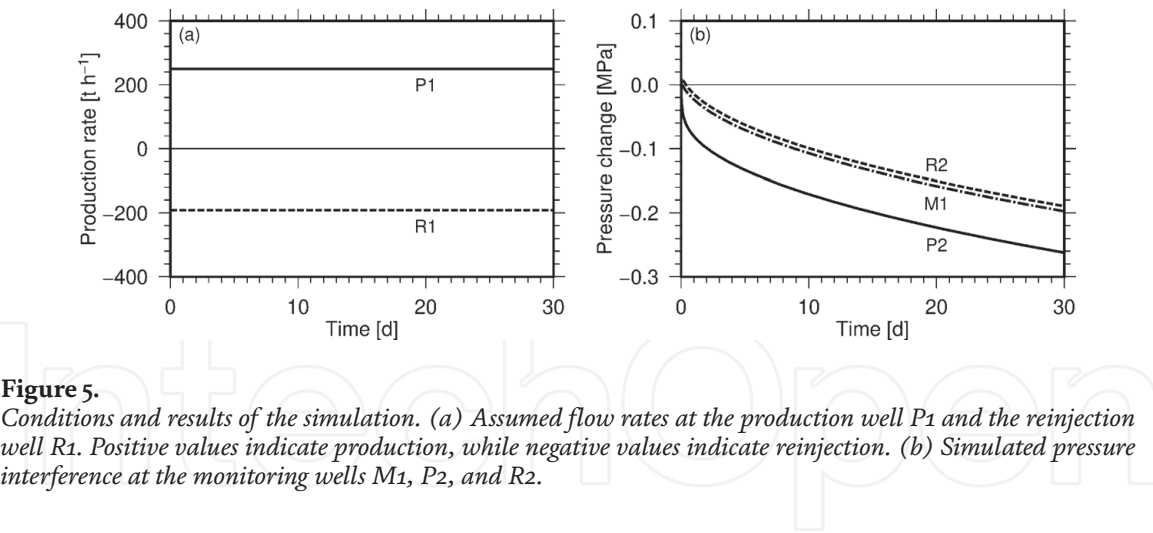
Figure 5.
Conditions and results of the simulation. (a) Assumed flow rates at the production well P1 and the reinjection well R1. Positive values indicate production, while negative values indicate reinjection. (b) Simulated pressure interference at the monitoring wells M1, P2, and R2.

4. Connecting wellbore flow and reservoir models

Next, a wellbore flow model is connected to the reservoir model; this is necessary to simulate and forecast future operational scenarios under specific conditions, such as a constant wellhead pressure. The author's numerical code implements this connection via two procedures. One is based on tabular data of the production rate depending on the feed zone pressure and the specific enthalpy. The other applies a highly refined local grid to simulate steep changes in the reservoir pressure around the wellbores.

Let us extend the reservoir model described in Section 3 by connecting it to a wellbore flow model. Using an appropriate wellbore flow simulation code (e.g., [9–14]), we assume that the production rate at a production well P1 with a constant wellhead pressure depends on the feed zone pressure and the specific enthalpy, as shown in **Figure 6**. Referring to the discretized tabular data, the code dynamically determines the production rate corresponding to arbitrary values of the pressure and the specific enthalpy via a bicubic interpolation. The reinjection rate at the reinjection well R1 is also dynamically determined by referring to the production rate at P1. Note that the code can only assume the steady-state wellbore flow represented by the tabular data. Simulating unstable transient wellbore flows, which is often a problem in operational power plants, connected to a reservoir model is a goal for future studies.

The pressure distribution covering the overall reservoir, including in the vicinities of wellbores, is simulated seamlessly using the highly refined local grids described in detail by [15]. The local grid defined around a wellbore enables steep pressure changes generated by production and reinjection at the well to be simulated by adopting grid
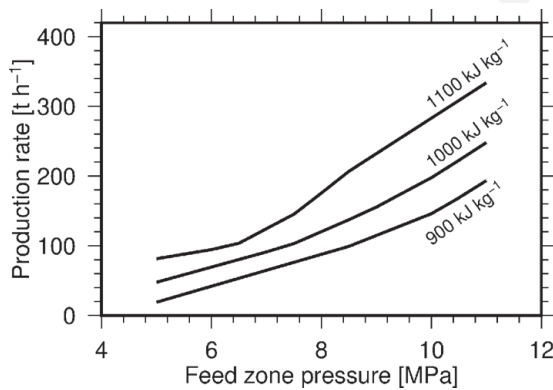

Figure 6.
Assumed production rate for the production well P1 depending on the feed zone pressure and the specific enthalpy.
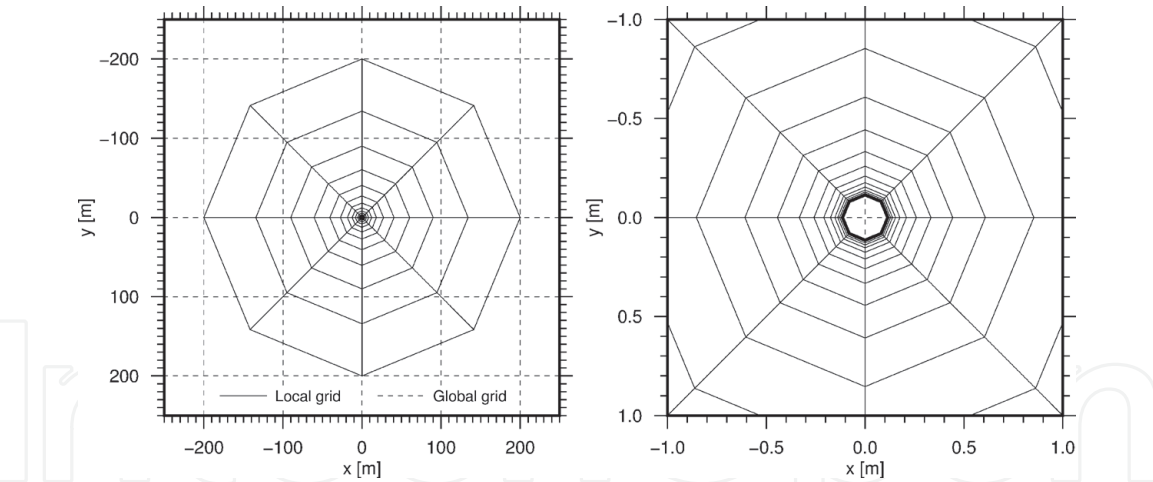
Figure 7.
Highly refined local grid around an 8.5-inch wellbore superimposed on a global grid shown on different scales.

sizes down to 1 mm, which is several orders of magnitude smaller than the size of the global grid covering the total planar porous medium. As shown in **Figure 7**, the ring-shaped local grid has external and internal boundaries. The variable values at the external boundary are dynamically determined by the values distributed in the global grid and are interpolated using a bilinear interpolation. Conversely, the variable values at the inner boundary corresponding to the wellbore surface are dynamically determined by the mass and enthalpy flow rates between the wellbore and the reservoir. When considering the skin effect, an extra pressure loss is considered between the internal boundary and the inside of the wellbore. When assuming the dependence of the production rate, as described in the previous paragraph, the production rate is determined as a solution of a coupled problem between this dependence and the fluid flow in the local grid. The determined production rate is referenced by the global grid to simulate the fluid flow in the global grid. Therefore, simulations in the global and local grids are dynamically coupled by referring to each other.

The simulated production and reinjection rates, as well as the pressure interference, using the extended model are shown in **Figure 8**. In this model, the production well P1 is equipped with tabular data for the production rate and a highly refined local grid assuming a hole size of 8.5 in. Selecting a value of 1.0 for the skin factor of P1, the simulated production and reinjection rates are similar to those assumed in the model described in Section 3. In fact, the production rate decreases gradually from 270.6 t h^{-1} to 243.0 t h^{-1} over the simulation period of 30 d. In this step of practical modeling connecting the wellbore and reservoir models, only the skin factors are
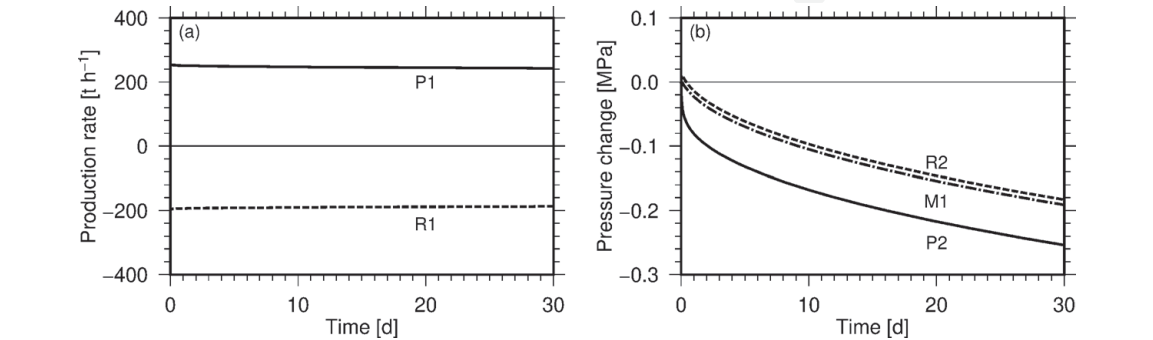

Figure 8.
Results of the simulation. (a) Simulated flow rates at the production well P1 and the reinjection well R1 using tabular data for the production rate and a highly refined local grid. Positive and negative values indicate production and reinjection, respectively. (b) Simulated pressure interference at the monitoring wells M1, P2, and R2.
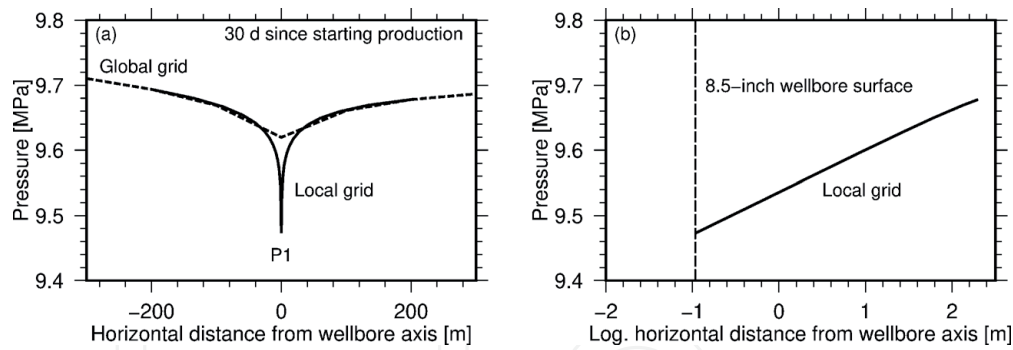
Figure 9.
Horizontal pressure distribution at the feed zone depth of the production well P1. (a) Pressure distribution on a linear scale simulated using the local grid (solid line) superimposed on that simulated using the global grid (broken line). (b) Pressure distribution on a logarithmic scale simulated using the local grid.

modified to match the simulated production rates with the observations, and the other parameter values of the planar porous media, such as permeability, thickness, and porosity, are maintained. In other words, the procedures in Sections 3 and 4 are straightforward.

The simulated pressure distribution around the production well P1 is shown in **Figure 9** on linear and logarithmic scales. The pressure distribution simulated using the local grid is smoothly connected to that simulated using the global grid and successfully reproduces a steep pressure drop in the vicinity of P1 (**Figure 9a**). On the logarithmic scale, it can be seen that the pressure increases proportionally to the logarithmic distance from the wellbore axis (**Figure 9b**), which is consistent with the solution of the problem assuming radial flow from a line-source adopted in the conventional well test analysis (e.g., [6]).

5. Estimating reservoir productivity

Finally, let us estimate the productivity of the above-discussed reservoir model by forecasting operational scenarios. We consider 15-year scenarios using the production wells P1 and P2, reinjection wells R1 and R2, and monitoring well M1. Both production wells obey the wellbore flow model described in the previous section. Forecasting scenarios for 15 years based on production tests for, at most, a few months involves uncertainty. We attempt to quantify this uncertainty by defining the surveyed and unsurveyed regions as illustrated in **Figure 4**.

Performing a longer production test, transient reservoir pressure responses are constrained by the wider spatial range reservoir properties, as discussed using the radius of investigation in the conventional well test analysis. We define the surveyed region as the region that constrains the simulated pressure responses when matching with observations, while the unsurveyed region is too distant to constrain the simulated pressure responses. Examining the effects of modifying the reservoir properties on the simulated pressure responses, the boundaries between the surveyed and unsurveyed regions are determined by trial and error. The boundaries move farther when performing longer production tests, indicating that the uncertainty in the forecasting scenarios becomes smaller. Note that defining the surveyed and unsurveyed regions, as well as extending the reservoir model to a huge horizontal distance, are symbolic parameterization methods for the uncertainty in terms of the transient pressure responses and do not include geological or other geoscientific insights.

Once we define the unsurveyed region, natural recharge and/or discharge over the boundaries between the surveyed and unsurveyed regions can be quantified
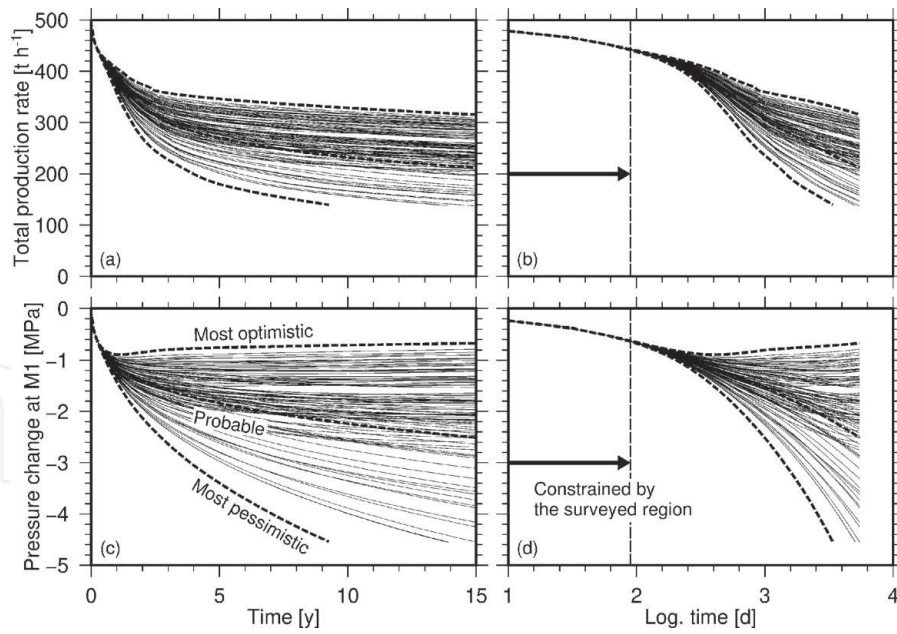
Figure 10.
Temporal changes in the total production rates at the production wells P1 and P2, as well as the pressure changes at the monitoring well M1, for 100 trial runs. Because the code is only capable of simulating single-phase reservoirs, runs whose reservoir pressure drops below the boiling pressure are terminated prior to 15 y.

using the permeability in the unsurveyed region as a symbolic parameter. Theoretically, the most optimistic case is to take the limit as the permeability approaches infinity, which is equivalent to assuming constant-pressure boundaries between the surveyed and unsurveyed regions. Conversely, the most pessimistic case is to set the permeability to zero, indicating impermeable boundaries. Modifying the permeability between zero and infinity, we can continuously control the magnitude of natural recharge and/or discharge. Even though, in the strictest sense, we have no information about the unsurveyed region, a probable case can be defined by giving the unsurveyed region the same permeability value as that in the surveyed region. All the parameters in the unsurveyed region, except the permeability, are assumed to be equal to those in the surveyed region.

In this chapter, we assume that the boundaries between the surveyed and unsurveyed regions are approximately 100 km from the wells (**Figure 4**). In the unsurveyed regions, the permeability values are randomly and independently selected in a range from 1.0×10^{-13} m^2 to 1.0×10^{-9} m^2 at each planar porous medium, while the permeability in the surveyed region is constant at 1.0×10^{-11} m^2. The probability distribution of the selection is assumed to be uniform in this range on a logarithmic scale. Under these conditions, temporal changes in the simulated total production rates from the two production wells P1 and P2, as well as the pressure changes at the monitoring well M1, for 100 trial runs are shown in **Figure 10**. For reference, the probable, most optimistic, and most pessimistic cases are also shown; these cases assume uniform permeability values in the unsurveyed regions of 1.0×10^{-11} m^2, 1.0×10^{-9} m^2, and 1.0×10^{-13} m^2, respectively. The simulated changes in the production rates and the reservoir pressures for all trial runs exhibit unique changes for approximately three months following the start of production. This indicates that the surveyed region extending 100 km from the wells constrains the changes during this period.

Summarizing the results of all the trial runs, we obtain monomodal frequency distributions for the production rates and the pressure changes, as shown in **Figure 11**. The medians of these distributions indicate a slightly more optimistic case (i.e., a larger production rate and a smaller pressure interference) than the probable case. This implies that a relatively high permeability value occurring in
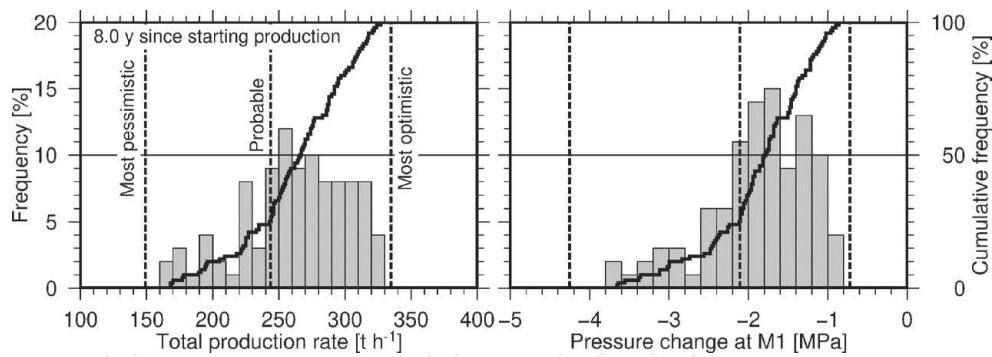
Figure 11.
Frequency distributions for the total production rates at the production wells P1 and P2, as well as the pressure changes at the monitoring well M1, after production for 8.0 y for 100 trial runs.

one unsurveyed region can result in a large overall reservoir productivity regardless of the low permeabilities in the other unsurveyed regions.

Accordingly, we obtain a present estimate of the reservoir productivity. Accounting for the power generation capacities corresponding to the forecasted production rates, the price of electricity, and the costs for the entire project, we can calculate the series of cash flows during the project period, as well as several profitability indices, such as the net present value and the internal rate of return. If the reservoir model is updated as a result of the in-parallel progress of the standard approach, the frequency distributions shown in **Figure 11** are also immediately updated via the procedures described in this chapter. The author mentions again and emphasizes that the new approach proposed in this chapter cannot stand alone because the standard approach, which exhaustively studies the geothermal system in terms of several geoscientific fields, is also essential. The combination of these approaches enables us to make the most of the limited time available during active explorational and developmental projects.

6. Forecasting temperature changes

Here, we briefly remark on forecasting temperature changes. As mentioned above, this chapter's approach aims to directly adhere to the observed transient responses as much as possible rather than referring to geological or other geoscientific interpretations. However, it is generally difficult to effectively forecast temperature changes in a reservoir over the decades of an assumed operational period. This is because promising prospects often do not exhibit detectable temperature changes at both production and monitoring wells during production tests. Even though tracer testing provides useful insights into advection from reinjection to production wells, it is not always sufficient to constrain the heat exchange efficiency between the fluid and the formation (i.e., it is not sufficient to determine the thickness of a planar porous medium, as mentioned in Section 3) while flowing in a reservoir.

To overcome this limitation, we need to develop measures to determine the heat exchange efficiency between the fluid and the formation rather than improve the modeling techniques. One possible technique may be to use dual tracers with different thermal resistivities, as proposed by [16]. The authors of that study proposed that temporal changes in the concentration ratio of a mixture of thermo-resistant and thermo-sensitive tracers depend on the temperature. Using this principle, we can monitor the temperatures experienced by reinjected fluid while it flows between the reinjection and production wells; this depends on the heat exchange efficiency between the reinjected fluid and the formation. A simulation from this viewpoint using dual tracers by [5] demonstrated the detection of two flow

paths with different temperatures in a reservoir. Another possible technique may be to perform a push-pull test, which compares the temperatures of injected and pumped-up fluids using a single well.

7. Conclusions

The author has developed an approach to estimate reservoir productivity under severe schedule limitations. Such limitations can originate from limited access to sites for drilling and well testing under snowy and mountainous conditions. To make the most of the limited time available, the new approach progresses in parallel with the conventional standard approach with an inverse approach using the transient responses observed while performing production tests, which are referenced in the final step of the standard approach. Combining these approaches, estimates of reservoir productivity can be rapidly generated. This feature is of value to successfully manage explorational and developmental projects.

Assuming a practical geothermal field, the author has demonstrated the procedures of this new approach. The procedures are straightforward: the pressure interference is simulated at the monitoring wells, the production and reinjection rates are simulated by combining the wellbore and reservoir models, then future operational scenarios are forecasted. By defining surveyed and unsurveyed regions, the reservoir model strictly divides the simulation period into an earlier period constrained by observations through the parameters in the surveyed region and a later period with no constraints. Performing a number of trial runs while randomly selecting permeability values in the unsurveyed regions, we can obtain frequency distributions for estimates of the reservoir productivity and successfully make project management decisions.

Acknowledgements

Author details

Mitsuo Matsumoto
Department of Earth Resources Engineering, Faculty of Engineering,
Kyushu University, Fukuoka, Japan

*Address all correspondence to: matsumoto@mine.kyushu-u.ac.jp

IntechOpen

References

[1] International Energy Agency Geothermal. 2019 IEA Geothermal Annual Report. Taupo: International Energy Agency Geothermal; 2020. 168 p.

[2] Grant, M.A., Bixley, P.F. Geothermal Reservoir Engineering. 2nd ed. Burlington: Academic Press; 2011. 378 p. DOI: 10.1016/C2010-0-64792-4

[3] DiPippo, R. Geothermal Power Plants: Principles, Applications, Case Studies and Environmental Impact. 2nd ed. Oxford: Butterworth-Heinemann; 2008. 520 p. DOI: 10.1016/B978-0-7506-8620-4.X5001-1

[4] Pruess, K., Oldenburg, C., Moridis, G. TOUGH2 user's guide, version 2. Berkeley: Lawrence Berkeley National Laboratory; 1999. 197 p. LBNL-43134. DOI: 10.2172/751729

[5] Matsumoto, M. A single-phase reservoir simulation method based on a roughly distributed and highly permeable fracture network model with applications to production and reinjection problems. Geothermics. 2020; 84: 101744. DOI: 10.1016/j.geothermics.2019.101744

[6] Dake, L.P. Fundamentals of Reservoir Engineering. Developments in Petroleum Science 8. Amsterdam: Elsevier; 1983. 462 p.

[7] Furuya, S., Aoki, M., Gotoh, H., Takenaka, T. Takigami geothermal system, northeastern Kyushu, Japan. Geothermics. 2000; 29: 191-211. DOI: 10.1016/S0375-6505(99)00059-0

[8] Goko, K. Structure and hydrology of the Ogiri field, West Kirishima geothermal area, Kyushu, Japan. Geothermics. 2000; 29: 127-149. DOI: 10.1016/S0375-6505(99)00055-3

[9] Miller, C.W. WELBORE user's manual. Berkeley: Lawrence Berkeley Laboratory; 1980. 48 p. LBL-10910. DOI: 10.2172/6334005

[10] Pritchett, J.W. WELBOR: a computer program for calculating flow in a producing geothermal well. La Jolla: S-Cubed; 1985. Report SSS-R-85-7283.

[11] Garg, S.K., Pritchett, J.W., Alexander, J.H. A new liquid hold-up correlation for geothermal wells. Geothermics. 2004; 33: 795-817. DOI: 10.1016/j.geothermics.2004.07.002

[12] Aunzo, Z.P., Bjornsson, G., Bodvarsson, G.S. Wellbore models GWELL, GWNACL, and HOLA. Berkeley: Lawrence Berkeley Laboratory; 1991. 102 p. LBL-31428. DOI: 10.2172/937440

[13] Pan, L., Oldenburg, C.M. T2Well—an integrated wellbore–reservoir simulator. Comput. Geosci. 2014; 65: 46-55. DOI: 10.1016/j.cageo.2013.06.005

[14] Matsumoto, M., Itoi, R., Fujimitsu, Y. Theoretical study of conditions for generation of periodic wellbore flow due to inflow of a lower-enthalpy fluid. Geothermics. 2021; 89: 101948. DOI: 10.1016/j.geothermics.2020.101948

[15] Matsumoto, M. Connecting wellbore and reservoir simulation models seamlessly using a highly refined grid. In: Proceedings of the 43rd Workshop on Geothermal Reservoir Engineering; 12-14 February 2018; Stanford. Stanford: Stanford University; 2018.

[16] Adams, M.C., Davis, J. Kinetics of fluorescein decay and its application as a geothermal tracer. Geothermics. 1991; 20: 53-66. DOI: 10.1016/0375-6505(91)90005-G